Syntheses, crystal structures, optical limiting properties, and DFT calculations of three thiophene-2-aldazine Schiff base derivatives†

Mohamed Ghazzali,[ad] Vratislav Langer,[a] Cesar Lopes,[b] Anders Eriksson[c] and Lars Öhrström*[a]

Received (in Montpellier, France) 16th March 2007, Accepted 1st June 2007
First published as an Advance Article on the web 28th June 2007
DOI: 10.1039/b704009a

The syntheses, characterizations and structural determinations of *N*,*N*′-bis(thiophenyl-2-methylene)hydrazine **1**, *N*,*N*′-bis(4-bromothiophenyl-2-methylene)hydrazine **2** and *N*,*N*′-bis(5-bromothiophenyl-2-methylene)hydrazine **3** are presented. The materials show third-order nonlinear behaviour with transmissions of 20, 22 and 18 μJ for an input energy of 150 μJ. The 4- and 5-bromothiophenic structures show Br···Br interactions of 3.562 and 3.626 Å, respectively. Analysis of bromine containing aromatic compounds in the Cambridge Crystallographic Database (CSD) showed the expected angle dependences of the Br···Br interactions dividing these into "type I" and "type II". A semi-quantitative agreement was found between the CSD data and a model derived form calculated electrostatic potentials.

Introduction

Bromine containing aromatic compounds have important applications on their own, a current issue is for example bromine containing flame retardants,[1] but are also versatile starting materials for the preparation of larger molecular units *via*, for example, Suzuki or Sonogashira couplings. Moreover, it has been realized that halogen substituents can form intermolecular bonds with various acceptor groups,[2] or even with other halogens,[3,4] thus rendering these compounds useful to the growing field of "crystal engineering".[5]

This article deals with the structural chemistry and intermolecular interactions of the two bromo-derivatives (Scheme 1) *N*,*N*′-bis(4-bromothiophenyl-2-methylene)hydrazine **2** and *N*,*N*′-bis(5-bromothiophenyl-2-methylene)hydrazine **3**, in particular the differences to the parent *N*,*N*′-bis(thiophenyl-2-methylene)hydrazine **1**. Specifically we will discuss the role of the Br···Br interaction in competition with other intermolecular forces.

We also discuss the C–Br···Br–C interaction in general, both by analysis of data in the Cambridge Crystallography Database and through quantum chemistry and simple models.

Moreover, we have earlier reported on the optical limiting (OL) properties for a number of thiophene–acetylene compounds,[6,7] and we include similar data for **1–3** in this study. In fact, **2** and **3** were prepared as versatile building blocks for OL materials and were not themselves expected to be highly active. However, a systematic study of the OL properties of thiophene-2-aldazines derivatives may increase the understanding of this phenomenon and help in the development of a rational approach to materials with optimized properties.

Results and discussion

Synthesis

Compounds **1–3** were synthesized adopting standard procedures[8] by condensation of thiophene-2-aldehyde, 4-bromothiophene carbaldehyde and 5-bromothiophene carbaldehyde, respectively, with hydrazine monohydrate giving yields of 79–88%.

Compound **2** is described here for the first time, while the preparation of compound **3** has been mentioned in preliminary reports only[9] and a complete characterization is given in the current communication. The parent compound *N*,*N*′-bis(thiophenyl-2-methylene)hydrazine **1** was prepared for reference purposes.

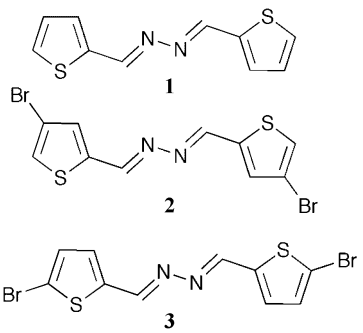

Scheme 1

[a] *Department of Chemical and Biological Engineering, Chalmers Tekniska Högskola, SE-412 96 Göteborg, Sweden. E-mail: mghazz@chalmers.se*
[b] *Department of Functional Materials, Swedish Defence Research Agency, SE-581 11 Linköping, Sweden*
[c] *Department of Laser Systems, Swedish Defence Research Agency, SE-581 11 Linköping, Sweden*
[d] *Department of Chemistry, Faculty of Science, Alexandria University, P.O.426, 21321 Alexandria, Egypt*

† Electronic supplementary information (ESI) available: Table S1 for bond lengths and Table S2 for bond angles for **1**, **2** and **3**, and DFT optimized coordinates for **1**, **2** and **3**. See DOI: 10.1039/b704009a

Table 1 Crystallographic, diffraction and structural refinement data for azine **1**, **2** and **3**, respectively

	1	**2**	**3**
Empirical formula	$C_{10}H_8N_2S_2$	$C_{10}H_6Br_2N_2S_2$	$C_{10}H_6Br_2N_2S_2$
Formula weight	220.30	378.11	378.11
Crystal system	Monoclinic	Monoclinic	Monoclinic
Space group	$P2_1/n$	$P2_1/c$	$P2_1/c$
a/Å	9.6504(7)	4.5456(2)	10.6766(6)
b/Å	11.4015(8)	26.9807(13)	11.5253(6)
c/Å	9.6510(7)	10.0137(5)	10.2713(6)
β/°	100.871(1)	97.484(1)	96.797(1)
V/Å^3	1042.83(13)	1217.65(10)	1255.01(12)
Z	4	4	4
F(000)	456	728	728
Crystal size/mm^3	0.28 × 0.18 × 0.16	0.92 × 0.19 × 0.02	1.10 × 0.18 × 0.12
θ range for data collection/°	2.15–33.04	2.19–33.03	2.61–25.37
Reflections collected	18997	21672	10951
Independent reflections	3775	4395	2298
R_{int}	0.0361	0.0359	0.0942
Max., min. transmission	0.9287, 0.8798	0.8732, 0.0602	0.4974, 0.0503
Data/restraints/parameters	3775/0/136	4395/0/151	2298/0/151
Goodness-of-fit on F^2	0.995	0.988	1.037
Final R indices [$I > 2\sigma(I)$]	$R1$ = 0.0346, $wR2$ = 0.0913	$R1$ = 0.0304, $wR2$ = 0.0730	$R1$ = 0.0490, $wR2$ = 0.1112
R indices (all data)	$R1$ = 0.0418, $wR2$ = 0.0974	$R1$ = 0.0416, $wR2$ = 0.0779	$R1$ = 0.0854, $wR2$ = 0.1259

Crystal structure analysis

It should be noted that the room-temperature crystal structure of **1** has been described earlier,[10] although the twinning phenomenon of the crystals was not recognized and consequently the data in this report are of significantly higher precision.

All three compounds crystallize in the same monoclinic space group and crystallographic data are summarized in Table 1.

The structure of azine **1** contains two crystallographic independent molecules A and B, each situated on an inversion centre and with almost no torsions in the chain (176–180°), and the two thiophene rings in each molecule are parallel, see Fig. 1. However, the mean planes defined by these two rings have inter-planar distances of 0.277 and 0.207 Å for A and B, respectively, thus the entire molecule cannot be described as truly planar.

The structure is twinned around a twofold axis and simulating a *C*-centred orthorhombic cell with a twinning ratio of 0.492(1)/0.508(1). The earlier report on this structure is qualitatively the same,[10] but by taking the twinning into account we have obtained a significantly higher precision, *i.e.* standard deviations of 0.002 Å, *vs.* 0.01 Å in ref. 10. Moreover, by treating the twining correctly artificially generated electron density peaks disappeared, thus removing doubts about the correctness, of the structure.

The intermolecular arrangements are not discussed in ref. 10 and are found to be a mixture of weak interactions, somewhat surprisingly excluding any significant π–π stacking. Instead the crystal is held together by numerous σ–π C–H to π interactions both from the rings and the chains (C–H···C 2.75–2.86 Å). As the ring–ring interactions (Fig. 2 right) are in the *c*-direction and the ring–chain interactions are in the *a*-direction (and propagated along the molecules in the *b*-direction) an intricate 3D pattern is formed, see Fig. 3. The C–H···S (3.27, 4.02 Å and 140°) and C–H···N (2.75, 3.50 Å and 138°) hydrogen bonds are very weak,[11] if at all significant, and sulfur–sulfur interactions are also absent. (In this and following paragraphs hydrogen bond interactions are presented as H···A and D···A distances and the D–H···A angle.)

In contrast to the molecular structure of **1**, in azine **2** the mean planes defined by the two thiophenes are no longer parallel having a dihedral angle of 5.67(10)° between them. The major reason for this is a torsion of the central N–N bond that now has a C═N–N═C angle of 175.88(17)° compared to 180.0° (enforced by symmetry) in **1**, see Fig. 4.

Neither in this structure is there any classical π–π stacking, however, another π–π stacking motif may be found as the thiophene rings and the C═N–N═C chain are stacked in a

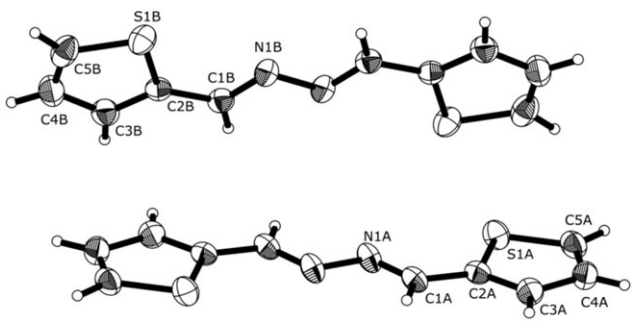

Fig. 1 ORTEP type diagram of **1**. Thermal ellipsoids are drawn at 50%.

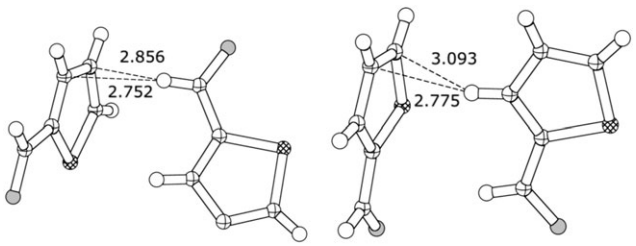

Fig. 2 The σ–π C–H to π interactions in **1**, left chain–ring and right ring–ring.

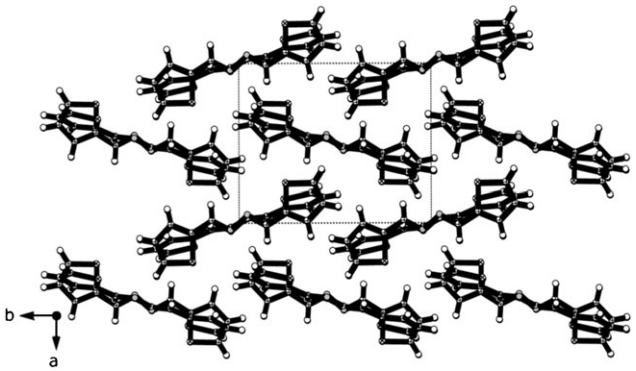

Fig. 3 Packing diagram of **1**.

staircase like way giving closest C···N and S···N distances of 3.378(3) and 3.502(3) Å, respectively. This may be due to the donor properties of the thiophene unit interacting with the acceptor character of the carbon–nitrogen double bond, see Fig. 5.

These stacks are interconnected by weak C–H···S (2.88 Å, 3.807 Å and 166.6°) hydrogen bonds but C–H···N (2.83, 3.362 Å and 117°) hydrogen bonds and sulfur–sulfur interactions are absent in this structure. However, there are also Br···Br interactions with a distance of 3.5618(4) Å between the bromine atoms, torsion angle (C–Br···Br–C) of 64.05° and angles (Br···Br–C) of 99.83° and 176.70° giving raise to zigzag chains along the *b*-axis, see Fig. 6.

The resulting structure has the staircase stacks propagating in the *c*-direction with neighbouring stacks having the molecular planes at 98° angles, see Fig. 7.

The molecular geometry of azine **3**, see Fig. 8, is distinctively none-planar with a angle of 20.1(3)° between the planes defined by the thiophene rings and a C=N–N=C torsion angle of 170.8(6)°. This can be compared to molecules of *N*,*N*′-bis(5-methylthiophenyl-2-methylene)hydrazine[12] with the corresponding plane–plane angle of 20.2° and a C=N–N=C torsion angle of 186.4°. There is also a seemingly longer N–N bond in **3** (1.410(8) Å) compared to 1.406(2)–1.403(2) in **1** and **2** but this difference is not significant (the corresponding distance in the methyl derivative is 1.408 Å[12]).

In compound **3**, (Fig. 8) finally, there is classical π–π stacking but only for one thiophene ring per molecule, see Fig. 9. The shortest atom–atom distance, C4A···S1A, is 3.707(8) Å and the two rings are perfectly parallel. Compared to **2** this gives a different packing pattern of the stacks propagating in the same direction, in the former case the Br···Br interaction gives a fish-bone pattern, in the case of **3** we get a 2D array of pair wise grouped azines. Also in this

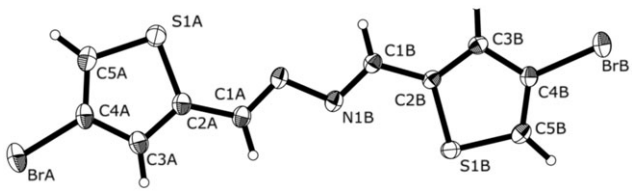

Fig. 4 ORTEP type diagram of **2**. Thermal ellipsoids are drawn at 50%.

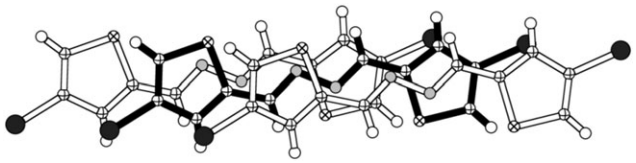

Fig. 5 Staircase like stacking of the thiophene rings and the C=N–N=C chain in **2**, giving closest C···N and S···N distances of 3.378(3) and 3.502(3) Å, respectively.

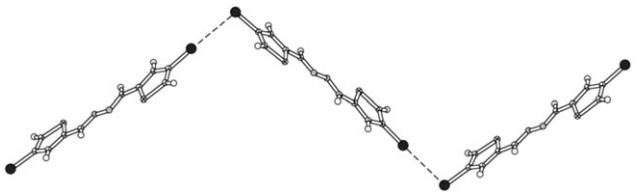

Fig. 6 Br···Br interactions in **2** shown perpendicular to the view in Fig. 5. This results in a fish-bone like pattern of the stacks.

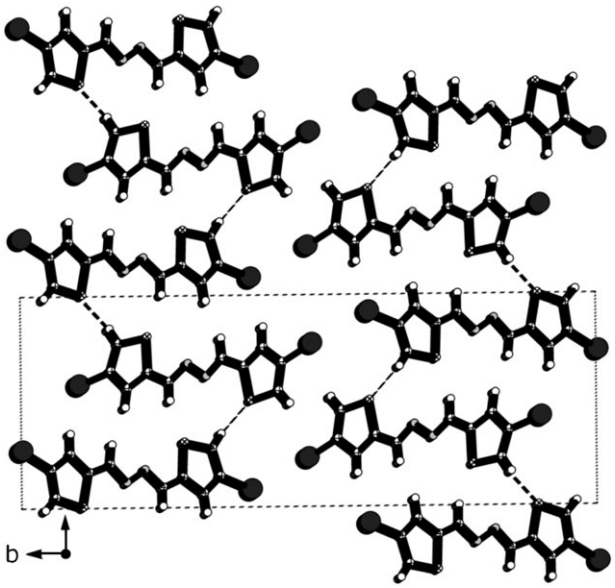

Fig. 7 Packing diagram of **2**, note that in neighbouring stacks the molecular planes make 98° angles towards each other. C–H···S hydrogen bonds are indicated with dashed lines.

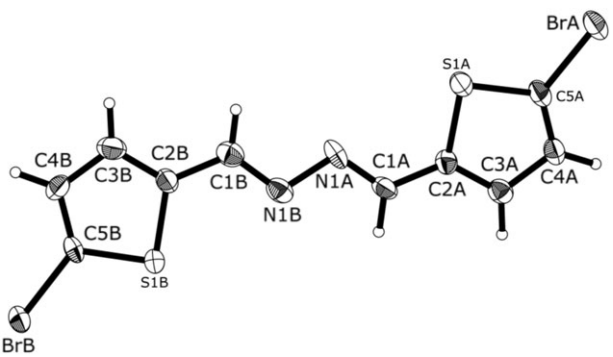

Fig. 8 ORTEP type diagram of **3**. Thermal ellipsoids are drawn at 50%.

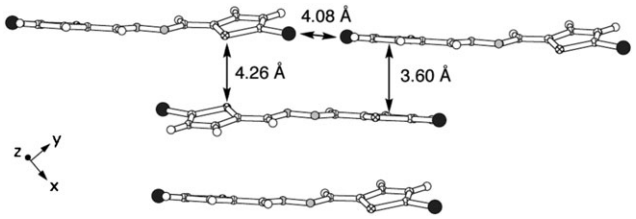

Fig. 9 Stacking interactions in **3**.

case, however, we get Br···Br interactions with a Br···Br distance of 3.626(1) Å, (C–Br···Br–C) torsion angle of 48.58° and angles (Br···Br–C) of 94.58° and 152.75°. This gives zigzag chains this time running at approximately 20° angle with the *a*-axis. In this compound, again the C–H···S interactions are very weak, closest H···S is 3.102 Å.

Similar to compound **2** the stacks, or in this case better the 2D array, has neighbouring stacks turned about 90°. Nevertheless, this similarity may not be significant as the two systems have quite different intermolecular interactions, see Fig. 10. The resulting packing diagram of **3** is found in Fig. 11.

In summary we can say that both substituents in 3- and 5-position will block the C–H···π interactions found in **1**, whereas the C–H···S interaction in **2** is blocked in **3** by replacing this hydrogen with a bromine.

Br···Br interactions

The nature of the interaction in the "halogen–halogen synthon" has recently been reviewed and found to be weakly attractive.[3] Estimates of intermolecular forces are always difficult and may vary largely from structure to structure, but available figures put the C–H···S hydrogen bond and the Br···Br interaction in the same range as the π–π stacking. This is not, however, uncontroversial as some studies indicate that the directionality instead comes from minimizing exchange repulsion forces.[13]

It may therefore be tempting to ascribe the difference in structures between the parent azine, **1**, and **2** and **3** as a consequence of this, as the same "synthon" is found in both structures. However, the 5-bromo derivative **3** is actually isostructural with the 5-methyl derivative reported in ref. 10, thus it is more likely that this interaction will only modulate the overall structure. In this case the $C–C_{Me}\cdots C–C_{Me}$ angles (153 and 160°) are changed to the 94.58 and 152.75° of the bromo derivative.

This prompted us to make a closer investigation of the C–Br···Br–C interactions of aromatic compounds. The type of Br···Br interaction found in **2** and **3** has been described in the literature as a "type-II interaction" and is predicted to have angles of $\theta_1 = 180°$ and $\theta_2 = 90°$ ($\theta_1 = C^1–Br^1\cdots Br^2$, $\theta_2 = Br^1\cdots Br^2–C^2$) because of the polarization (anisotropy) of the bromine electron density.[14] The "type-I" interactions have $\theta_1 = \theta_2$ and are usually $>110°$. This is illustrated by the calculated electrostatic potentials (see DFT section for details) for the 5-bromothiophene monomer in Fig. 12.

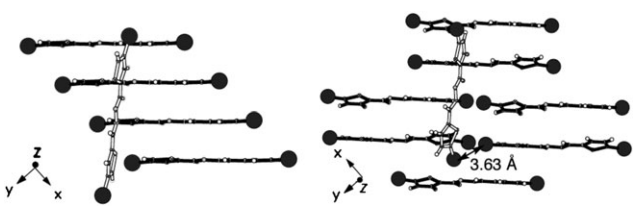

Fig. 10 Comparing the perpendicular arrangements in **2** and **3**.

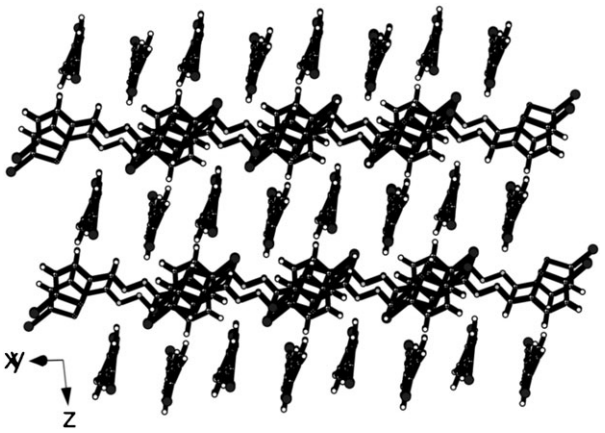

Fig. 11 Packing diagram of **3**.

We have substantiated this by an analysis of the Br···Br interactions in bromine substituted aromatic compounds in the Cambridge Structural Database.[15] 1018 not-disordered hits were found with 4049 Br···Br distances shorter than 5 Å. These were divided into three groups: (1) interactions smaller than twice the van der Waals radii (r_{vdW}) (3.6 Å); (2) distances between 3.6 and 4.0 Å (attractive interaction may occur up to this value) and (3) Br···Br distances longer than 4 Å.

A histogram showing the number of hits *vs.* distances is displayed in Fig. 13 and a maximum can be seen at roughly $2r_{vdW} + 0.4$ Å.[16]

In Fig. 14 θ_1 has been plotted against θ_2 and clear differences can be seen between the three different Br···Br subsets.

For shorter interactions we have roughly as many hits on the diagonal as off, and the diagonal hits, "type I", are centred around 140–160° in qualitative agreement with Awwadi *et al.*[3]

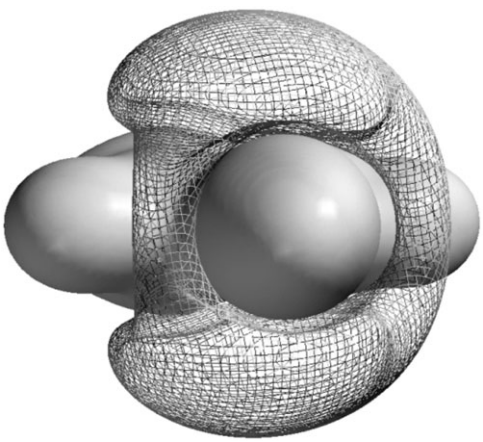

Fig. 12 Surfaces with isoelectrostatic potentials for 5-bromothiophene calculated by DFT. Solid surface has +10 eV and mesh surface has −10 eV. The view has the bromine atom pointing outwards toward the viewer and the molecular plane is horizontal.

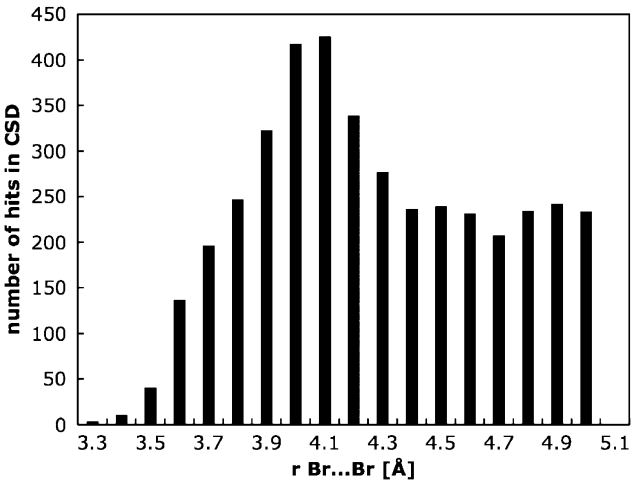

Fig. 13 Br···Br interactions in aromatic compounds in the CSD.

The off diagonal hits occur preferentially in the region θ_1: 150–180° and θ_2: 80–125° and are thus of "type II".

For the intermediate region the spread is larger, and half the hits fall on the diagonal. This time these are centred around 130–150° but with a prominent peak also at 70–110°. The off-diagonal hits show a trend of $\theta_1 + \theta_2 = 180°$. These cases correspond to π–π stacking with parallel C–Br bonds intersecting the skew-axis of the stacking (typically 100–120°) giving the geometrical relation of $\theta_1 = 180° - \theta_2$. The other off-diagonal hits show a weak trend of a type II behaviour in the region θ_1: 130–180° and θ_2: 70–125°.

Finally, in the upper region of Br···Br distances where we do not really expect any interactions the π–π stacking effect is dominant.

While this study supports the proposed "type-II interaction" model, it also indicates that other factors may be more important for the overall structure. Indeed, it is highly likely that a large proportion of the studied compounds contain other important supramolecular "synthons" such as weak or strong hydrogen bonds. For the present compounds, the Br···Br interaction is at interplay with the σ–π C–H to π interactions found in **1** and the π-interactions and C–H···S hydrogen bonds in **2** and **3**, and in the case of **3** it seems clear that it is only responsible for a minor modulation of the overall structure.

Computational studies

Computing the intermolecular interactions accurately is a difficult theoretical problem that needs to involve high levels of theory such as MP2, and large basis sets, and such calculations are still relatively expensive. However, we expect the workhorse of molecular computations, density functional theory (DFT), to give a good picture of the electrostatic potential around a molecule. This could then be used to gain a qualitative understanding of the interaction.

The electrostatic iso-surfaces were presented in Fig. 12 and based on this we can make a simple model. We reduce the problem to two dimensions by cutting vertically through the bromide atom in Fig. 12 and assume that the electron density is still approximately spherical. We will then have a central larger positive region with a width of about the radius of the circle and peripheral regions of negative polarisation.

We can then discern the two ways of obtaining contacts between negative and positive parts corresponding to the type I and type II interactions mentioned before, see Fig. 15.

This picture explains the type I and type II interactions, but there is nothing especially new in this. However, with this model we can also compute the preferred angles θ_1 and θ_2. Type I should thus have $\theta_1 = \theta_2 = 150°$ and type II should have $\theta_1 = 180°$ and $\theta_2 < 120°$. This is in agreement with the CSD data analysis. Moreover, the observation of relatively more type II interactions at shorter distances (about half the hits) may perhaps be understood by considering what will happen if the two spheres are pushed into each other. For type I this will immediately give repulsion as same sign potentials meet. On the contrary, for type II we can push the spheres a considerable distance into each other before repulsion takes place.

A couple of other features of these systems can be tackled theoretically: We observe a substantial torsion around the N–N bond in **3** and a survey of the CSD indicates that this is rare (5 out of 31 compounds have this angle >2°). This "flatness" should be due to the partly double bond character of this bond. However, we do not see a significant elongation

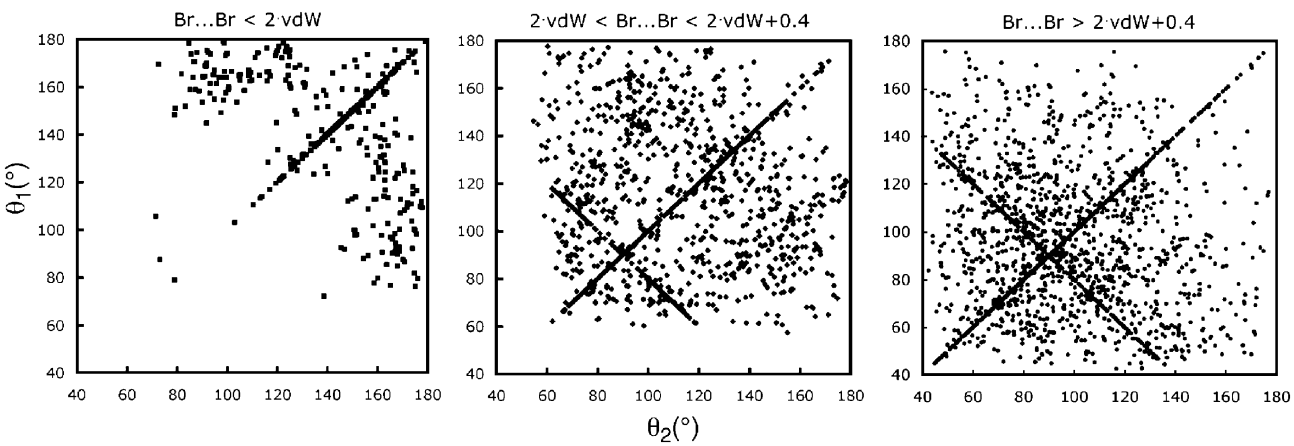

Fig. 14 The C–Br···Br–C angles θ_1 and θ_2 for the three different Br···Br criteria: left; interactions smaller than twice the van der Waals radii (3.6 Å). **2**. Middle; distances between 3.6 and 4.0 Å (attractive interaction may occur up to this value) and right; Br···Br distances longer than 4 Å.

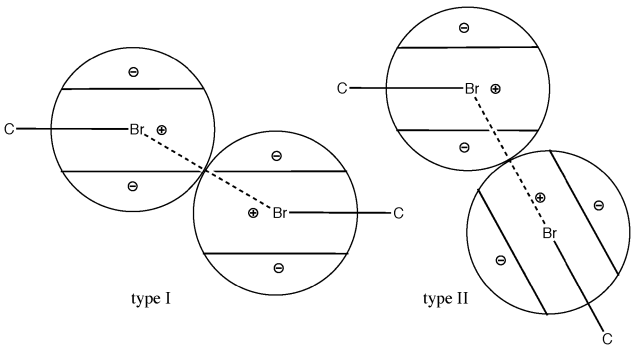

Fig. 15 Simple 2D model of the Br···Br interaction based on the electrostatic potentials in Fig. 12.

of the N–N bond in the X-ray structure. Thus, we wanted to predict the magnitude of this change.

We also wanted to know about the HOMO–LUMO structure of these compounds and how they are affected by the substitution in different positions.

Full geometry optimizations were performed on all molecules, and in addition a restricted optimization was run on **3** with three dihedral angles frozen so as to retain the deformation found in the crystal structure. For the 5-F and 5-Cl derivatives **3b–3c** of the 5-Br azine **3**, only halogen–carbon distances were optimized starting from the fully optimized structure of **3**.

As expected, all calculated structures are completely planar and torsion free, thus indicating that the substantial torsions in **2** and **3** are the effect of intermolecular interactions. The torsion is primarily found around the N–N bond and thus should be related to the bond-order of this bond, formally of order one. However, substantial delocalization will increase the double bond character of the N–N interaction, and indeed for the crystal structure of thiophene **1** the N–N bond lengths are in between the double bond (1.20 Å) and the single bond (1.50 Å). As the experimental evidence of a bond length increase was non-conclusive we also optimized a molecule **3a** with the three torsion angles along the chain frozen at the X-ray values. This structure gave an N–N length of 1.377 Å, significantly (on the computational level) longer that the 1.373 Å found for the completely optimized planar structure, and an energy difference to this conformer of +6 kJ mol^{-1}. Indeed, this difference is within our experimental standard deviations and too small to be detected by the most precise X-ray measurements.

Fig. 16 shows the HOMOs and LUMOs for **1–3**. Small but significant differences are noted between the compounds; thus the contribution of bromine lone pair orbitals to HOMO and LUMO in **2** is much smaller than in **3**, that also has completely lost the sulfur character of the HOMO. This gives a stronger antibonding nature to the HOMO orbital and, consequently, a higher energy resulting in a lower HOMO–LUMO energy gap (as the LUMOs are more alike). Moreover, this effect depended on the strong polarizability of the bromine atom or a better match of orbital energies, as is shown by complementary calculations on the 5-F and 5-Cl derivatives **3b** and **3c** (Fig. S2, ESI†). These sets of results show an increasing halogen contribution to the HOMO as the atomic number is increased. (The major molecular orbital coefficients for the halogens in the HOMO increase from 0.21 with F to 0.29 with Br.)

Thus, if an electronic effect is desired on the HOMO–LUMO system, a substitution in the 5-position will be more efficient than in the 4-position.

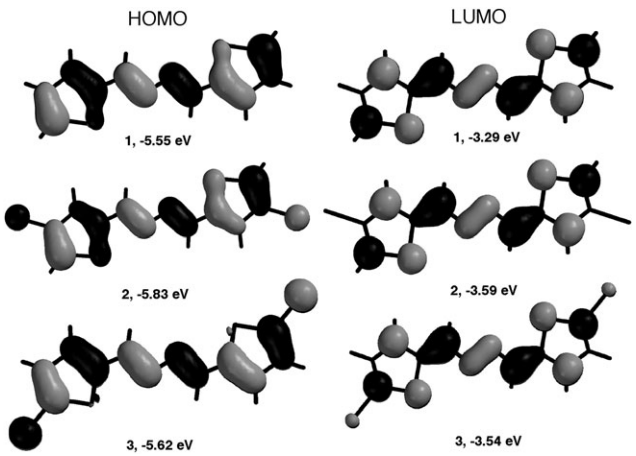

Fig. 16 HOMO and LUMO DFT "molecular orbitals" and their energies for **1**, **2** and **3**, respectively.

Optical limiting measurements

The possibility to change the intensity of laser radiation in a predetermined and predicted manner is one of the most fundamental challenges in optics science. Since Maiman[17] invented the first intense light beam based on a laser source, the need for protection against this highly coherent radiation has triggered research at different levels.[18]

An ideal optical power limiting (OPL) material, attenuates the transmitted intensity of laser radiation to some specific safe values. At the same time, the material should exhibit high transmittance for normal light. Thus, such a material has nonlinear properties.[19]

As a part of our efforts to find such self-activating laser radiation power limiters we have earlier reported results for a number of thiophene–acetylene compounds.[6,7] We are now investigating thiophene-2-aldazines as these could easily be

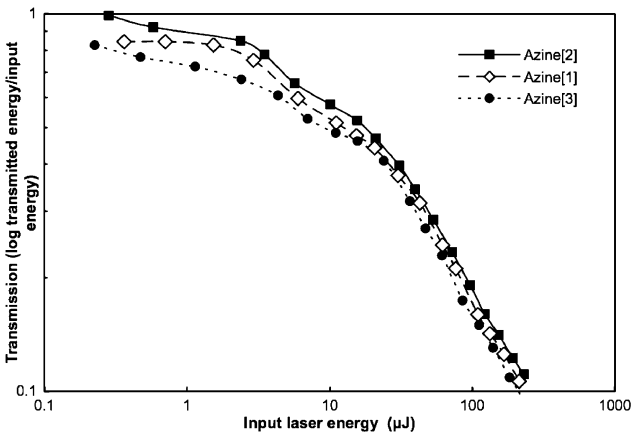

Fig. 17 Nonlinear transmission of **1–3** (50 mM in THF).

conjugated with other classes of molecules (Pt–acetylene complexes,[20] porphyrines[7,21]) to prepare new OL materials.

Even though no great effect was expected for **2** and **3** a systematic study of the OL properties of different derivatives and building blocks may increase the understanding of this phenomenon and help in the development of a rational approach to materials with optimized properties.

Fig. 17 shows the nonlinear optical behaviour of the compounds in a logarithmic diagram. The input laser energy is shown on the *X*-axis and the resulting transmittance ($\log(I_{out}/I_{in})$) of the solution has been plotted on the *Y*-axis. For an ideal optical limiting material the transmittance should approach zero for high input energies.

This is not the case for these compounds. However, the materials show third-order nonlinear behaviour with transmitted energies of 20, 22 and 18 μJ for an input laser energy of 150 μJ. These values are comparable to what has been obtained for other, more elaborate, thiophene derivatives (8–36 μJ), and thus encourage further studies of these compounds.[6,7]

It was also found that **3** has the highest linear absorption in this study and this is in agreement with the frontier orbital energy description as the presence of bromine atoms in the position 5 implies an existence of a stronger electronic interaction at molecular level compared to **2** with bromine atoms at the position **4**.

Conclusions

The structures of aldazines **1–3** were found to depend on many weak intermolecular interactions with no single type being common or decisive in the three structures. The "type II" Br···Br interactions were, however, found in both brominated aldazines and play a structural role in these compounds.

Moreover, the Br···Br interactions in aromatic bromine substituted compounds could be explained by a simple model based on the calculated electrostatic potentials and semi-quantitative agreement is found between this model and an analysis of data from the CSD.

The optical power limiting properties of **2** and **3** indicate that they may be used as versatile starting materials for more extensive π-conjugations at the position of the peripheral bromine atoms using Suzuki coupling conditions to improve both chemical and optical properties.

Experimental

Methods and instrumentation

The IR spectra were recorded in the region 4000–400 cm^{-1} using spectroscopic grade KBr-pellet method on Bruker IFS66 v/S with resolution of 8 cm^{-1} and 64 scans, the aperture opening was 12 mm with a double sided acquisition mode function. ^1H and ^{13}C NMR spectra were recorded on a Varian UNITY-400 at ambient temperature using the $CDCl_3$ residual $CHCl_3$ peak as internal reference. Melting points were measured on Mettler FP-90 Hot Stage thermoanalyser and were not corrected. The non-linear absorption experiments were performed by an *f*/5 set up[22] with a frequency-doubled Nd:YAG laser operating at 10 Hz, delivering 10-ns pulse widths. The transmittances of 50 mM solutions of **1–3** in THF were measured in 2 mm Quartz cells.

Search of the Cambridge Crystallography Database

Compounds in the Cambridge Crystallography Database, CSD, version 5.27, November 2006 were searched.[15] Only organic structures were retrieved, and these were error and disorder free with *R*-values lower than 10% and restricted to bromides attached to a carbon having aromatic bonds to its neighbours.

Materials

Hydrazine monohydrate and the thiophene carbaldehydes corresponding to products **1–3** were purchased from Aldrich. Solvents employed were of analytical reagent grade and were used without further purifications. Analytical thin-layer chromatography (TLC) was carried out using Merck silica gel 60 plates. Single crystals of **1–3** suitable for X-ray diffraction were obtained by slow evaporation of a methanol (99.5%) solution of the respective compound over a period of 1 month.

Syntheses

N,*N*′-Bis(thiophenyl-2-methylene)hydrazine **1**, *N*,*N*′-bis(4-bromothiophenyl-2-methylene)hydrazine **2** and *N*,*N*′-bis(5-bromothiophenyl-2-methylene)hydrazine **3** were synthesized adopting standard procedures[8,23] by condensation in an 95%-ethanolic solution of thiophene-2-aldehyde, 4-bromothiophene carbaldehyde and 5-bromothiophene carbaldehyde, respectively (40 mmol) with hydrazine monohydrate (20 mmol). The resulting solutions were heated under reflux for 3–4 h and then a gradual cooling produced crystalline yellow solids that were separated by filtration, washed by diethyl ether and dried *in vacuo* giving yields of 81.5% (96% in ref. 10), 87.5 and 79%, respectively; mp 150 °C (148–149 °C in ref. 10 and 153 °C in ref. 16), 144 and 146 °C, respectively.

^1H, ^{13}C NMR (δ/ppm, $CDCl_3$) and IR (ν/cm^{-1}, KBr) for **1** were found to be in good agreement with reported data.[10] For *N*,*N*′-bis(4-bromothiophenyl-2-methylene)hydrazine **2** we report: IR (ν, cm^{-1}, KBr): 509 (w), 590 (s, ν_{CBr}), 698 (w), 725 (m), 735 (m), 769 (w), 830 (m), 880 (m), 950 (m), 1180 (m), 1230 (m), 1280 (s), 1345 (m, $\nu_{C=S}$), 1410 (s), 1500 (s), 1550 (w), 1605 (s, $\nu_{C=N}$), 1660 (w), 1700 (w), 1740 (w), 1900 (w), 2330 (w), 2350 (w), 2950 (w), 3100 (s), 3743 (w). ^1H NMR (δ, ppm, $CDCl_3$): 8.66 (s, 2H), 7.40 (s, 2H), 7.30 (s, 2H). ^{13}C NMR (δ, ppm, $CDCl_3$): 111 (s, 2H), 127.6 (s, 2H), 134.5 (s, 2H), 140 (s, 2H), 155 (s, 2H). Correspondingly for *N*,*N*′-bis(5-bromothiophenyl-2-methylene)hydrazine **3**: IR (ν, cm^{-1}, KBr): 485 (m), 590 (s, ν_{CBr}), 678 (w), 745 (m), 785 (m), 1060 (m), 1200 (m), 1230 (m), 1265 (w), 1385 (s, $\nu_{C=S}$), 1410 (s), 1500 (w), 1550 (m), 1605 (s, $\nu_{C=N}$), 1660 (w), 1735 (w), 1876 (w), 2094 (w), 2455 (w), 2938 (w), 3060 (s), 3743 (w). ^1H NMR (δ, ppm, $CDCl_3$): 8.60 (s, 2H), 7.15 (s, 2H), 7.06 (s, 2H). ^{13}C NMR (δ, ppm, $CDCl_3$): 118.6 (s, 2H), 129.5 (s, 2H), 131 (s, 2H), 140.7 (s, 2H), 155.4 (s, 2H).

Crystallography

Diffraction data were collected using a Siemens SMART CCD diffractometer with Mo-Kα radiation (λ = 0.71073 Å, graphite monochromator). The crystals were cooled to 173(2) K by a flow of nitrogen gas using the LT-2A device. Full spheres of reciprocal space were scanned by 0.3° steps in ω with a crystal-to-detector distance of 3.97 cm. Preliminary orientation matrices were obtained from the first frames using SMART.[24] The collected frames were integrated using the preliminary orientation matrices which were updated every 100 frames. Final cell parameters were obtained by refinement of the positions of reflections with $I > 10\sigma(I)$ after integration of all the frames using SAINT software.[24] The data were empirically corrected for absorption and other effects using the SADABS program.[25] The structures were solved by direct methods and refined by full-matrix least squares on all $|F^2|$ data using SHELXTL software.[26] For compound **1** [*N*,*N*′-bis(thiophenyl-2-methylene)hydrazine] we initially obtained unreasonably high residuals and residual electron density, thus an investigation of possible twinning was made. As the unit cell parameters a = 9.6504 Å and c = 9.6510 Å were very close to each other, the twinning law (0 0 −1 0 −1 0 −1 0 0) was successfully employed with resulting 0.5084(13) to 0.4916(13) ratio.

CCDC reference numbers 609791–609793 for **1**, **2** and **3**, respectively.

For crystallographic data in CIF or other electronic format see DOI: 10.1039/b704009a

Computational details

Calculations were made with the DFT module in Spartan 5.1.3a1[27] at using the exchange and correlation functionals of Becke[28] and Perdew,[29] respectively (BP86) as a perturbation on self consistent density. A DN** basis set including polarization and *d*-functions for C, N, O, S and Br was used. This basis set is roughly equivalent in "size" to the 6-31G** basis set but is claimed to yield results closer to much larger Gaussian basis sets.[30]

Acknowledgements

This work was supported by the Swedish Research Council and the Swedish International Development Agency-SIDA through the Swedish Research Links program (VR-Grant 348-2002-6879).

References

1 B. Hileman, *Electron. Waste Chem. Eng. News*, 2006, **84**(1), 18–21.
2 (*a*) P. Metrangolo, G. Resnati, T. Pilati, R. Liantonio and F. Meyer, *J. Polym. Sci., Part A: Polym. Chem.*, 2007, **45**, 1–15; (*b*) P. Metrangolo, T. Pilati and G. Resnati, *CrystEngComm*, 2006, **8**, 946–947.
3 F. F. Awwadi, R. D. Willett, K. A. Peterson and B. Twamley, *Chem.–Eur. J.*, 2006, **12**, 8952–8960.
4 (*a*) F. Zordan, L. Brammer and P. Sherwood, *J. Am. Chem. Soc.*, 2005, **127**, 5979–5989; (*b*) M. Fourmigue and P. Batail, *Chem. Rev.*, 2004, **104**, 5379–5418.
5 (*a*) D. Braga, L. Brammer and N. R. Champness, *CrystEngComm*, 2005, **7**, 1–19; (*b*) D. Braga, *Chem. Commun.*, 2003, 2751.
6 P. Lind, A. Eriksson, C. Lopes and B. Eliasson, *J. Phys. Org. Chem.*, 2005, **18**, 426–433.
7 R. Vestberg, C. Nilsson, C. Lopes, P. Lind, B. Eliasson and E. Malmström, *J. Polym. Sci., Part A: Polym. Chem.*, 2005, **43**, 1177–1187.
8 A. Garg and J. P. Tandon, *Transition Met. Chem.*, 1988, **13**, 395.
9 A. A. El-Emam, M. A. Moustafa, H. M. Eisa and M. M. El-Kerdawy, *Heterocycles*, 1986, **24**, 1025.
10 C.-J. Lin, W.-S. Hwang and M. Y. Chiang, *J. Organomet. Chem.*, 2001, **640**, 85.
11 T. Steiner, *Angew. Chem., Int. Ed.*, 2002, **41**, 48–76.
12 C. J. Lin, W. S. Hwang and M. Y. Chiang, *Polyhedron*, 2001, **20**, 3275–3280.
13 S. L. Price, A. J. Stone, J. Lucas, R. S. Rowland and A. E. Thornley, *J. Am. Chem. Soc.*, 1994, **116**, 4910–4918.
14 (*a*) C. M. Reddy, M. T. Kirchner, R. C. Gundakaram, K. A. Padmanabhan and G. R. Desiraju, *Chem.–Eur. J.*, 2006, **12**, 2222; (*b*) G. R. Desiraju and R. Parthasarathy, *J. Am. Chem. Soc.*, 1989, **111**, 8725; (*c*) V. R. Pedireddi, D. S. Reddy, B. S. Goud, D. C. Craig, A. D. Rae and G. R. Desiraju, *J. Chem. Soc., Perkin Trans. 2*, 1994, 2353.
15 F. H. Allen, *Acta Crystallogr., Sect. B*, 2002, **58**, 380.
16 For a discussion of the relationship between intermolecular distance and intermolecular energy, see for example: I. Dance, *New J. Chem.*, 2003, **27**, 22–27.
17 T. H. Maiman, *Nature*, 1960, **187**, 493.
18 B. Anderberg and M. L. Wolbarsht, *Laser Weapons: The Dawn of a New Military Age*, Plenum Press, New York, 1992.
19 P. N. Prasad and D. J. Williams, *Introduction to Nonlinear Optical Effects in Molecules and Polymers*, Wiley, New York, 1991.
20 (*a*) R. Vestberg, R. Westlund, A. Eriksson, C. Lopes, M. Carlsson, B. Eliasson, E. Glimsdal, M. Lindgren and E. Malmstrom, *Macromolecules*, 2006, **39**, 2238–2246; (*b*) C. Desroches, C. Lopes, V. Kessler and S. Parola, *Dalton Trans.*, 2003, 2085–2092.
21 (*a*) R. B. Martin, H. P. Li, L. R. Gu, S. Kumar, C. M. Sanders and Y. P. Sun, *Opt. Mater.*, 2005, **27**, 1340–1345; (*b*) M. Calvete, G. Y. Yang and M. Hanack, *Synth. Met.*, 2004, **141**, 231–243.
22 (*a*) D. Vincent and J. Cruickshank, *Appl. Opt.*, 1997, **36**, 7794; (*b*) D. Vincent, *Sect. B: Nonlinear Opt.*, 1999, **21**, 413.
23 N. R. El-Rayyes and A. H. Katrib, *J. Chem. Eng. Data*, 1983, **28**, 132.
24 J. Tao, X. Yin, Y. B. Jiang, R. B. Huang and L. S. Zheng, *Inorg. Chem. Commun.*, 2003, **6**, 1171–1174.
25 SADABS: Program for Empirical Absorption Correction of Area Detectors, Version 2.10, University of Göttingen, Germany, 2003.
26 SHELXTL: Structure Determination Programs, Version 6.12, Bruker AXS Inc., Madison, WI, USA, 2001.
27 SPARTAN '04, Ver. 1.0.3e, Wavefunction Inc., 18401 Von Karman Avenue, Suite 370. Irvine, CA 92612, USA, 2006.
28 A. D. Becke, *Phys. Rev. A*, 1988, **38**, 3098–3100.
29 J. P. Perdew, *Phys. Rev. B*, 1986, **33**, 8822–8824.
30 W. J. Hehre, J. Yu and P. E. Klunzinger, *A Guide to Molecular Mechanics and Molecular Orbital Calculations in Spartan*, Wavefunction, Inc., 1997.

